frontiers in Pharmacology

ORIGINAL RESEARCH
published: 28 July 2021
doi: 10.3389/fphar.2021.732540

The miR-130a-3p/TGF-βRII Axis Participates in Inhibiting the Differentiation of Fibroblasts Induced by TGF-β1

Yanhong Liu[1], *Yan Ding*[1], *Yapeng Hou*[1], *Tong Yu*[1], *Hongguang Nie*[1] *and Yong Cui*[2]*

[1]Department of Stem Cells and Regenerative Medicine, College of Basic Medical Science, China Medical University, Shenyang, China, [2]Departments of Anesthesiology, The First Hospital of China Medical University, Shenyang, China

Pulmonary fibrosis (PF) is a chronic progressive interstitial lung disease that has a poor prognosis. Abnormal activation of transforming growth factor-β1 (TGF-β1) plays a crucial role in fibroblast differentiation. Mesenchymal stem cells (MSCs) are currently being considered for the treatment of PF, but the regulatory mechanisms are poorly understood. We co-cultured bone marrow-derived MSCs and mouse lung fibroblasts (MLg) in the presence of TGF-β1, and studied the protein/mRNA expression of fibrosis markers and related signaling pathways. The effects of miR-130a-3p and TGF-β receptor II (TGF-βRII) on the differentiation of MLg induced by TGF-β1 were studied using immunofluorescence assay, Western blot, and quantitative real-time PCR techniques, respectively. Our results showed that MSCs reversed the overexpression of fibrosis markers and TGF-β1/Smad signaling pathway proteins and mRNAs after TGF-β1 treatment and increased the level of miR-130a-3p. TGF-βRII was identified as a target of miR-130a-3p and was evaluated by dual-luciferase reporter assay. The miR-130a-3p/TGF-βRII axis could suppress the differentiation of lung fibroblasts *via* the TGF-β1/Smad signaling pathway, thereby reducing the process of PF.

Keywords: pulmonary fibrosis, mesenchymal stem cells, mouse lung fibroblast, microRNA, TGF-β1

OPEN ACCESS

Edited by:
Jian Gao,
Second Affiliated Hospital of Dalian Medical University, China

Reviewed by:
Hongwei Yao,
Brown University, United States
Xiangming Ji,
Georgia State University, United States

***Correspondence:**
Yong Cui
cynhg@cmu.edu.cn

Specialty section:
This article was submitted to Respiratory Pharmacology, a section of the journal Frontiers in Pharmacology

Received: *29 June 2021*
Accepted: *19 July 2021*
Published: *28 July 2021*

Citation:
Liu Y, Ding Y, Hou Y, Yu T, Nie H and Cui Y (2021) The miR-130a-3p/TGF-βRII Axis Participates in Inhibiting the Differentiation of Fibroblasts Induced by TGF-β1. Front. Pharmacol. 12:732540. doi: 10.3389/fphar.2021.732540

INTRODUCTION

Pulmonary fibrosis (PF) is a chronic lung disease, and its incidence has been rising in recent years (Wu and Xu, 2020; Li et al., 2021). PF usually affects elderly patients, and radiation and mechanical or chemical stimulation have become the main risk factors associated with PF (Froidure et al., 2020; Jin et al., 2020; Yang et al., 2020). The main pathological features of PF are alveolar epithelial cell damage, fibroblast proliferation and activation, excessive collagen deposition, and a large accumulation of extracellular matrix (Sauler et al., 2019; Zhi et al., 2020). Transforming growth factor-β1 (TGF-β1) regulates proliferation and differentiation in a multitude of cell types, and TGF-β1/Smad signaling pathway is associated with fibrosis (Barrett et al., 2017; Liu et al., 2020; Wnuk and Paw, 2020). TGF-β1 binds to TGF-β receptor II (TGF-βRII) on the cell surface, which recruits TGF-βRI. Activation of the latter can phosphorylate Smad2/3 and associates with Smad4, which translocates from the cytoplasm to the nucleus, and regulate gene transcription (Yoshida et al., 2018; Wang et al., 2021).

Abbreviations: miRNAs, microRNAs; MLg, mouse lung fibroblast; MSCs, mesenchymal stem cells; PF, pulmonary fibrosis; qRT-PCR, quantitative real-time PCR; TGF-β1, transforming growth factor-β1; TGF-βRII, TGF-β receptor II.

Mesenchymal stem cells (MSCs) were first discovered and isolated from bone marrow and have multilineage differentiation and self-renewal capacity (Li and Wu, 2020). MSCs are able to promote cell proliferation, repair tissue damage, and improve the microenvironment of the lung tissue *via* extracellular vesicle release to deliver DNA, mRNA, and microRNAs (miRNAs) (Behnke et al., 2020; Kavianpour and Saleh, 2020; Li et al., 2020). Stem cell-derived miRNAs have recently been found to regulate various cellular processes, such as proliferation, apoptosis, stress responses, differentiation, and angiogenesis. Recent literature has shown the potential roles of miRNAs, a type of small noncoding RNA in PF (Dutta et al., 2019; Boateng and Krauss-Etschmann, 2020; Cho et al., 2020), which can regulate target genes or proteins through inflammatory responses related to mRNA degradation or translation inhibition. Among these miRNAs, miR-130a-3p observed in MSCs has been reported to have antitumor effects and has been used for treating neurological diseases (Chen et al., 2010; Glaesel et al., 2020; Zhong et al., 2020). It has also been found that miR-130a-3p could exert cardioprotective effects through the induction of angiogenesis in ischemic hearts after myocardial infarction (Moghaddam, et al., 2019). In the bleomycin-treated mouse PF model, miR-130a-3p mimics significantly reduced the macrophage profibrogenic gene expression (Su et al., 2015). However, studies focused on miR-130a-3p functions in fibroblasts are seldom published. In this study, we investigated bone marrow MSC (BMSC)-derived miR-130a-3p and co-cultured it with mouse lung fibroblasts (MLg) to explore its expression and regulatory mechanism in PF.

By analysis and prediction using TargetScan and miRanda software, we found that miR-130a-3p and TGF-βRII are potential binding partners, the latter of which is important for the TGF-β1 signaling pathway (Kushibiki et al., 2005). We speculate that BMSC-derived miR-130a-3p may participate in the TGF-β1/Smad signaling pathway to inhibit the differentiation of lung fibroblasts, which provides an effective therapeutic approach for PF prevention and treatment by targeting TGF-βRII.

MATERIALS AND METHODS

BMSC Culture and Co-Cultured With MLg

The male C57 mice (weight 9–10 g) were provided by China Medical University, and all experiments were performed with the research protocol approved by the Ethics Committee of China Medical University (No. CMU2019088). According to the method previously reported, BMSCs were isolated and cultured in DMEM/F12 medium with 10% fetal bovine serum (FBS, Gibco, United States), 10 ng/ml recombinant mouse basic fibroblast growth factor (PeproTech, United States), 1% penicillin/streptomycin, and maintained at 37°C in 5% CO_2 (Hou et al., 2020). The medium was changed every 2 days. BMSC characterization has been confirmed in our previously published paper (Zhou et al., 2021). At 80% confluence, the medium of BMSCs was changed with DMEM/F12 medium without FBS. BMSC-CM was collected after 24 h and stored at −80°C. MLg was purchased from American Type Culture Collection (ATCC, United States) and cultured in a 6-well plate with DMEM medium adding 10% fetal bovine serum (FBS, Gibco, United States), and 1% penicillin/streptomycin. For the co-culture mode, the BMSCs were prepared in 6-well Transwell inserts, which were transferred to the 6-well plate with MLg seeded at the bottom after 24 h. The BMSCs co-cultured with MLg were treated with DMEM without FBS for another 24 h, and used for the following experiment.

Cell Transfection

BMSCs or MLg was transfected using Lipofectamine 2000 (GenePharma, CHN) according to the manufacturer's protocol. In brief, 50–60% confluent BMSCs or MLg grown in medium was incubated with Lipofectamine 2000 reagent and TGF-βRII-siRNA (si-TGF-βRII), miR-130a-3p mimic (Mimic), miR-130a-3p inhibitor (Inhibitor), negative control (NC, the negative control of miR-130a-3p mimic or si-TGF-βRII), and inhibitor NC (the negative control of miR-130b inhibitor) for 72 h, respectively. Labeled CY3-miR-130a-3p was also used and its distribution was observed under a fluorescence microscope.

Western Blot Assays

MLg was washed three times with PBS and lysed using a cell lysis reagent. Proteins were analyzed by SDS-PAGE (10% polyacrylamide gels) and transferred to PVDF membranes (Invitrogen, United States). Membranes were blocked with 5% BSA for 1 h and incubated with primary antibodies, which were against α-SMA (Merck, GER; 1:1,000 dilution), FN (Abcam, United States; 1:1,000 dilution), TGF-βRII (Elabscience, CHN; 1:1,000 dilution), SMAD2/3 (Elabscience, CHN; 1:1,000 dilution), p-SMAD2/3 (Elabscience, CHN; 1:1,000 dilution), and β-actin (Santa Cruz, United States; 1:1,000 dilution). The membranes were then washed three times with TBST and incubated with goat anti-rabbit or anti-mouse secondary antibody (ZSGB-BIO, CHN; 1:5,000 dilution) at room temperature for 1 h. The bands of protein were obtained from the same membrane, which were then visualized using an ECL kit on a Tanon-5200 chemiluminescence detection system (Tanon, CHN) and quantified using ImageJ program.

Quantitative Real-Time PCR Analysis

According to the manufacturer's instructions, total RNA was isolated using TRIzol reagent (Invitrogen, United States) and the extracted RNA samples were quantified by NanoDrop 2000C spectrophotometer (Thermo, United States). Total RNA and miRNAs were reverse transcribed into cDNA using synthesis Kit (TaKaRa, Japan). Quantitative real-time PCR (qRT-PCR) reactions were then performed with SYBR Premix Ex Taq II (TaKaRa, Japan) in the ABI 7500 System. Results were calculated using the GAPDH (for mRNAs) or U6 gene (for miRNAs) (Santa Cruz Biotechnology, United States) as internal controls based on the $2^{-\Delta\Delta CT}$ method. All the primers are shown in **Table 1**.

Cell Viability Assay

The effects of miR-130a-3p and si-TGF-βRII on MLg viability were measured by CCK8 assay (Dojindo, CHN) according to the manufacturer's instructions. Briefly, MLg were cultured in a 96-

TABLE 1 | Primer sequences of qRT-PCR.

Gene	Forward primer sequence	Reverse primer sequence
α-SMA	5′-CTA TGA AGG CTA TGC CCT GCC-3′	5′-GCT TCT CCT TGA TGT CTC GCA C-3′
FN	5′-TGT TAT GGA GGA AGC CGA GGT T-3′	5′-CGA TGC AGG TAC AGT CCC AGA-3′
Col III	5′-TGG AAA CTG GGG AAA CAT GC-3′	5′-GGA TTG CCG TAG CTA AAC TGA-3′
TGF-βR I	5′-AAA CTT GCT CTG TCC ACG G-3′	5′-AAT GGC TGG CTT TCC TTG-3′
TGF-βR II	5′-GTA ATA GGA ATG CCC ATC CAC-3′	5′-GAT TTC TGG TTG TCA CAG GTG-3′
SMAD2	5′-AGA ATA TCG GAG GCA GAC AG-3′	5′-GTT ACA GCG AGT CTT TGA TGG-3′
GAPDH	5′-AGA AGG CTG GGG CTC ATT TG-3′	5′-AGG GGC CAT CCA CAG TCT TC-3′
U6	5′-GGA ACG ATA CAG AGA AGA TTA GC-3′	5′-TGG AAC GCT TCA CGA ATT TGC G-3′
miR-130a-3p	5′-CAG UGC AAU GUU AAA AGG GCA U-3′	5′-GCC CUU UUA ACA UUG CAC UGU U-3′

well plate along with NC, miR-130a-3p, or si-TGF-βRII, respectively. After 24 h, TGF-β1 (5 μl) was added to the corresponding well. 48 h after incubation, 10% CCK8 solution was added to each well. After the cells were incubated for additional 2 h, the absorbance was measured at 450 nm wavelength with a microplate reader (Tecan, CH).

Immunofluorescence Staining for α-SMA

MLg was incubated in 6-well plates, and fixed for 30 min with 4% of paraformaldehyde (Sigma, GER). After washing, 0.1% Triton X-100 was used for permeabilization. The cells were then visualized using anti-α-SMA primary antibody (CBL171, Mreck, GER; 1:200 dilution) at 4°C overnight and a labeled secondary antibody for 90 min. The nuclei were stained for DAPI for 15 min in the dark. Finally, the cells were examined using a fluorescence microscope.

Dual Luciferase Reporter Gene Assay

The wild-type (WT) TGF-βRII 3′-untranslated regions (3′-UTR) and mutant-type (MUT) TGF-βRII (3′-UTR) sequences of TGF-βRII were synthesized by GenePharma (CHN). The miR-130a-3p mimic or miR-130a-3p negative control was cotransfected into H441 cells using Lipofectamine 2000. After 48 h, luciferase activities were detected by the Dual Luciferase Reporter Assay Kit (Vazyme, CHN).

Statistical Analysis

All data were processed by Origin 8.0 and presented as the mean ± SE. Normality and homoscedasticity test were done by Levene and Shapiro-Wilk test before applying parametric tests. The differences between two groups was determined by Student's two-tailed *t*-test. When the data did not pass the normality or homoscedasticity test, non-parametric *t*-test (Mann-Whitney *U*-test) was applied. $p < 0.05$ was regarded as statistically significant.

RESULTS

BMSCs Rescues TGF-β1-Induced Myofibroblast Differentiation *In Vitro*

TGF-β1 is involved in the development of PF. Some studies have shown that the inhibition of proliferation and differentiation of fibroblasts are related to the activation of TGF-β1, and the signaling pathways mediated by it play a vital role in lung diseases (Wolters et al., 2014; Aschner and Downey, 2016). The PF model was constructed by treating MLg with 10 ng/mL TGF-β1 for 24 h, which in some case was also added just after MLg was co-cultured with BMSCs. The Western blot assay revealed that the levels of fibrosis markers (α-SMA and FN) in MLg increased after TGF-β1 treatment, whereas the expression levels reduced when co-cultured with BMSCs (**Figures 1A–C**), indicating a successful PF *in vitro* model with TGF-β1-induction. Subsequently, we assessed the expression levels of the above indicators with qRT-PCR, and the result was consistent with that of the Western blot (**Figures 1D–F**). These data suggest that BMSCs significantly rescued TGF-β1-induced myofibroblast differentiation.

Aberrant transcription of signaling pathways might trigger PF, among which TGF-β1 plays a central role (Saito et al., 2018a; Froidure et al., 2020). As expected, TGF-β1/Smad signaling pathway proteins (TGF-βRII, SMAD2/3 and p-SMAD2/3) increased with TGF-β1 treatment, which was reversed after BMSC administration (**Figures 2A–C**), and verified at the mRNA level (**Figures 2D–F**). This observation indicates that the TGF-β1/Smad signaling pathway may participate in the beneficial effect of BMSCs in PF.

BMSCs Enhance the Expression Level of miR-130a-3p After TGF-β1 Induction

It is well known that miRNAs can help MSCs communicate with their surrounding environment (Asgarpour et al., 2020). We hypothesized that the role of BMSCs in TGF-β1-induced fibroblasts may be mediated *via* miRNAs. Based on relevant literature reports and website prediction, we screened out miR-130a-3p that may be beneficial to PF, which was present both in MSCs and MSCs-derived microparticles (Chen et al., 2010; Ferguson, et al., 2018). BMSC-CM is a medium that contains the secretions in BMSCs, such as exosome, miRNAs, etc (Marlina, et al., 2021). We postulated that BMSCs may participate in the protective effects on PF by secreting miR-130a-3p to BMSC-CM and then exert its effects on the receptor cell MLg, and to verify this possibility, we compared the content of miR-130a-3p originating from MLg, BMSC, and BMSC-CM, which showed higher expression levels in BMSC than in BMSC-CM (**Figure 3A**). Moreover, miR-130a-3p significantly decreased after TGF-β1 induction compared with the control group, which was reversed after BMSC administration, suggesting that miR-130a-3p might be related to BMSC treatment of PF (**Figure 3B**).

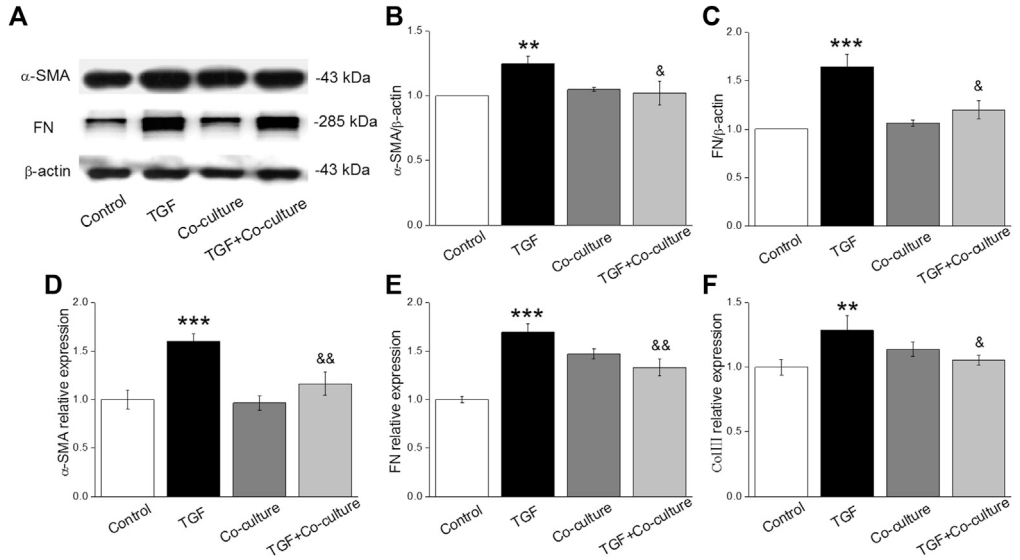

FIGURE 1 | TGF-β1 treatment enhances the level of fibrotic-related protein/mRNAs and BMSCs reverse the above expression in MLg. **(A)** Representative bands of α-SMA and FN protein expression by Western blot in MLg treated with TGF-β1 for 24 h and/or co-cultured with BMSCs for 24 h **(B,C)** Statistical analyses were showed with relative gray values of the protein bands (α-SMA/β-actin and FN/β-actin). **(D-F)** Representative statistical analysis of α-SMA, FN and Col III mRNA by qRT-PCR (α-SMA/GAPDH, FN/GAPDH and Col III/GAPDH). Data were presented as mean ± SE, $^{**}p < 0.01$, $^{***}p < 0.001$, compared with Control group. $^{\&}p < 0.05$, $^{\&\&}p < 0.01$, compared with TGF group. n = 3–6.

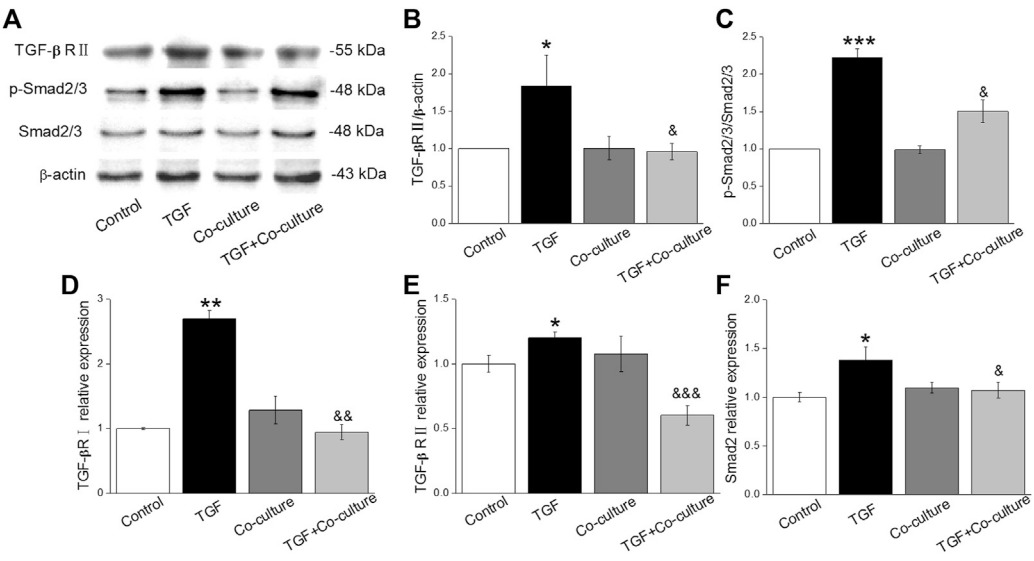

FIGURE 2 | BMSCs decrease the level of TGF-β1/Smad signaling pathway proteins in MLg treated with TGF-β1. **(A)** Representative bands for TGF-βRII, Smad2/3, and p-Smad2/3 protein levels. **(B,C)** Statistical analyses were obtained from relative gray values of the protein bands (TGF-βRII/β-actin and p-Smad2/3/Smad2/3). **(D-F)** Representative statistical analysis of TGF-βRI, TGF-βRII and Smad2 mRNA by qRT-PCR (TGF-βRI/GAPDH, TGF-βRII/GAPDH and Smad2/GAPDH). Data were presented as mean ± SE, $^{*}p < 0.05$, $^{**}p < 0.01$, $^{***}p < 0.001$, compared with Control group. $^{\&}p < 0.05$, $^{\&\&}p < 0.01$, $^{\&\&\&}p < 0.001$, compared with TGF group. n = 3–4.

MiR-130a-3p Inhibits Fibroblast Differentiation

Increasing evidence indicates that both the proliferation and differentiation of fibroblasts contribute to the formation of fibrosis, and TGF-β1 stimulates fibrotic-related α-SMA expression, collagen synthesis, and extracellular matrix deposition (Li et al., 2016; Huang et al., 2017). To confirm the effect of miR-130a-3p, we transfected MLg with the miR-130a-3p mimic and then added TGF-β1 after 48 h. Above all, the CCK8 assay results showed that TGF-β1 significantly promoted the

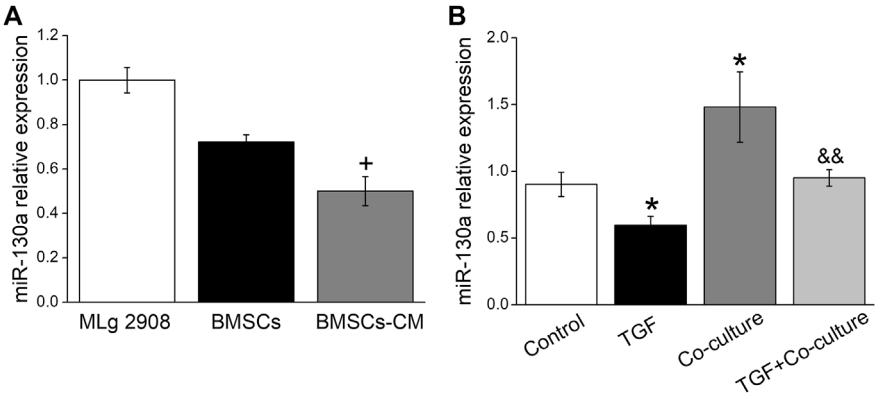

FIGURE 3 | The expression of miR-130a-3p *in vitro*. **(A)** The expression of miR-130a-3p in MLg, BMSCs and BMSCs-CM was detected by qRT-PCR (miR-130a-3p/U6). **(B)** The expression of miR-130a-3p in MLg treated with TGF-β1 for 24 h and/or co-cultured with BMSCs for 24 h $^{+}p < 0.05$, compared with BMSCs group. $^{*}p < 0.05$, compared with Control group. $^{\&\&}p < 0.01$, compared with TGF group. $n = 3$.

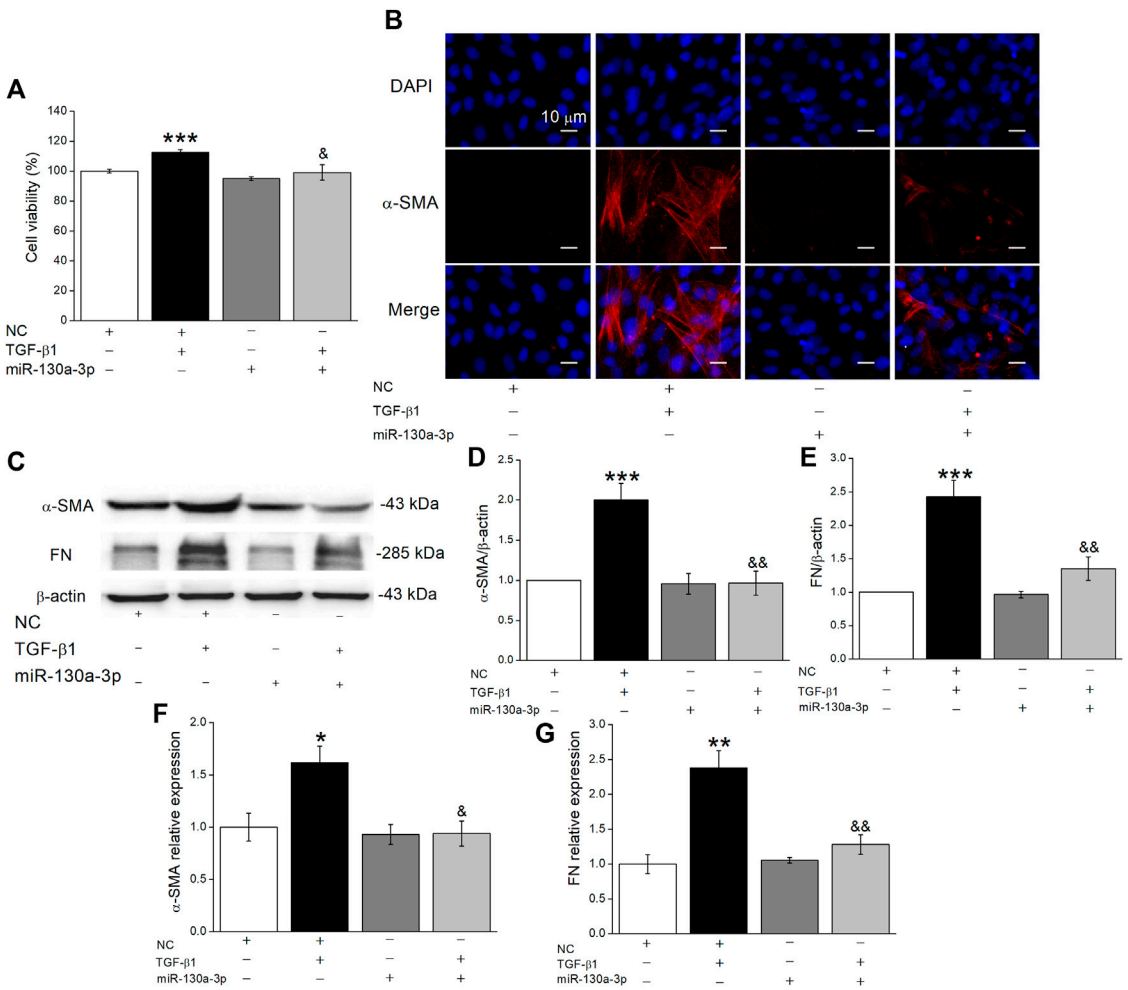

FIGURE 4 | The effect of miR-130a-3p on the differentiation in TGF-β1-induced MLg. **(A)** The relative cell viability was measured in CCK8 assay, and the data for NC group was set to 100%. **(B)** The effect of miR-130a-3p on fibroblast-myofibroblast transition was measured with immunofluorescence. Scale bar = 10 μm. **(C)** Western blot bands of α-SMA and FN protein expression in MLg after transfection of miR-130a-3p. **(D,E)** Statistical analyses were obtained from relative gray values of the protein bands (α-SMA/β-actin and FN/β-actin). **(F,G)** The result of qRT-PCR assay shows the α-SMA and FN mRNA level in MLg (α-SMA/GAPDH, and FN/GAPDH). Data were presented as mean ± SE, $^{*}p < 0.05$, $^{**}p < 0.01$, $^{***}p < 0.001$, compared with NC group. $^{\&}p < 0.05$, $^{\&\&}p < 0.01$, compared with NC + TGF group. $n = 3$–5.

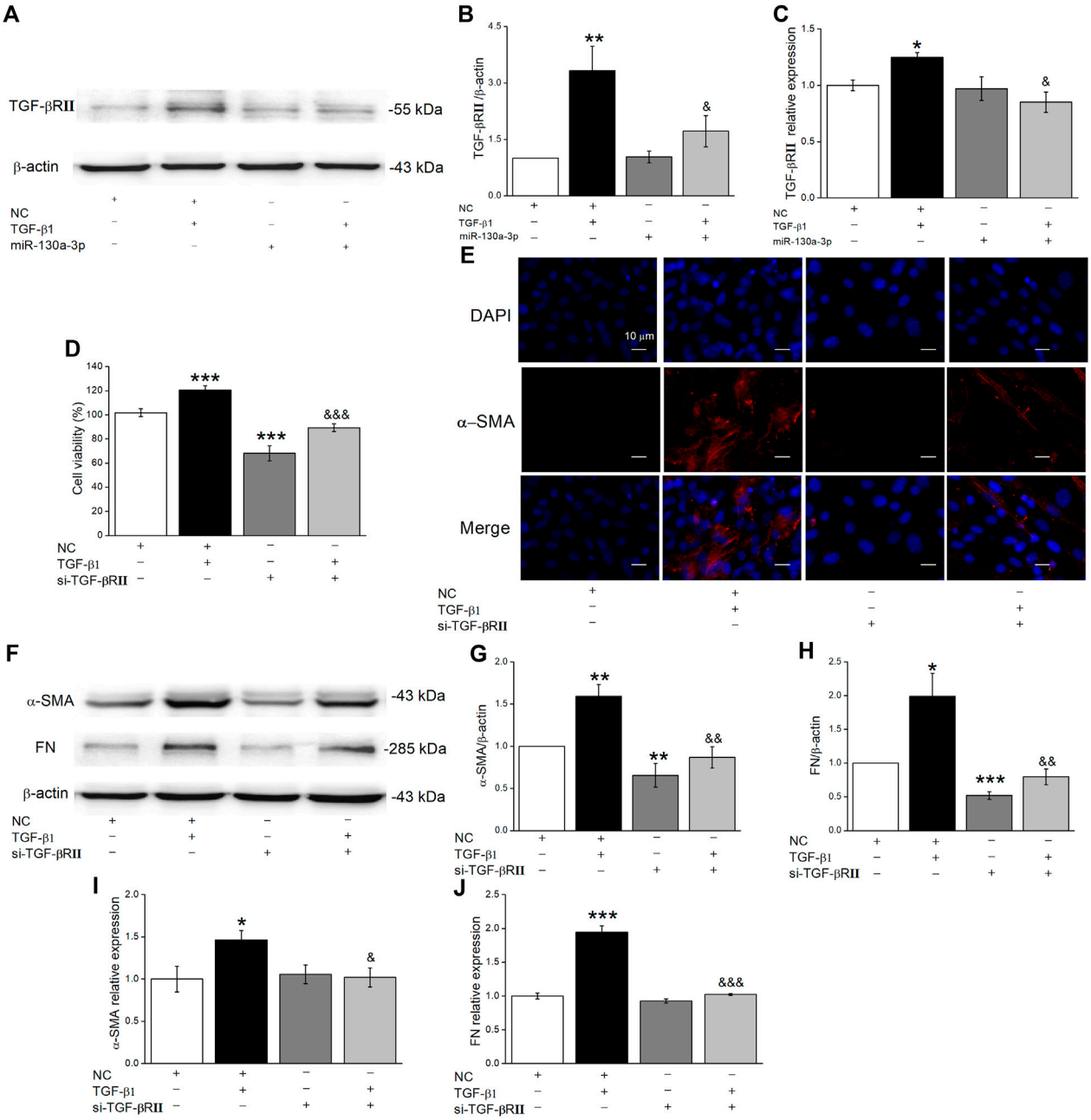

FIGURE 5 | MiR-130a-3p decreases protein level TGF-βRII in MLg and silencing TGF-βRII inhibits TGF-β1-induced MLg differentiation. **(A)** Representative Western blot bands of TGF-βRII protein expression in MLg transfected with miR-130a-3p mimic and treated with TGF-β1 for 24 h. **(B)** Level of TGF-βRII protein was obtained from Western blot analysis. **(C)** Level of TGF-βRII mRNA was analyzed. **(D)** The effect of TGF-βRII knockdown on the inhibition of MLg proliferation. **(E)** Immunofluorescence staining was demonstrated the effect of TGF-βRII silence on MLg differentiation. Scale bar = 10 μm. **(F)** Western blot bands of α-SMA and FN protein expression in MLg after transfection of si-TGF-βRII. **(G,H)** Western blot statistical analyses for α-SMA and FN protein (α-SMA/β-actin and FN/β-actin). **(I,J)** qRT-PCR statistical analyses for α-SMA and FN mRNA (α-SMA/GAPDH and FN/GAPDH). Data were presented as mean ± SE, $^{*}p < 0.05$, $^{**}p < 0.01$, $^{***}p < 0.001$, compared with NC group. $^{\&}p < 0.05$, $^{\&\&}p < 0.01$, $^{\&\&\&}p < 0.001$, compared with NC + TGF group. $n = 3–4$.

viability in MLg, which was inhibited by miR-130a-3p (**Figure 4A**). Meanwhile, the immunofluorescence results showed that overexpression of miR-130a-3p inhibited the differentiation of MLg, which was enhanced after TGF-β1 stimulation (**Figure 4B**). Consistently, TGF-β1 upregulated the expression of fibrotic-related proteins and mRNAs in MLg, which was reversed by the miR-130a-3p mimic (**Figures 4C–G**). Taken together, these results indicate that miR-130a-3p is involved in the regulation of fibroblast differentiation.

TGF-βRII is a Target Gene of miR-130a-3p

Gene targets of miR-130a-3p were identified using miRNA target prediction databases, and we found that TGF-βRII was a possible target gene of miR-130a-3p. Previous studies showed that the TGF-β1 signaling pathway controls cell proliferation, differentiation, organ development, etc., by combing with TGF-βRII (Shi et al., 2020). First, we examined whether miR-130a-3p downregulated TGF-βRII expression by Western blot and qRT-PCR (**Figures 5A–C**). Moreover, to explore whether miR-130a-3p suppresses the differentiation of MLg by deregulating TGF-βRII, we researched the influence of silencing TGF-βRII on the differentiation of MLg. Using the CCK8 assay, we found that si-TGF-βRII could inhibit the viability of MLg induced by TGF-β1, indicating that TGF-βRII plays an indispensable role in the TGF-β1 signaling pathway (**Figure 5D**). Simultaneously, si-TGF-βRII was further verified to inhibit differentiation in MLg according to an immunofluorescence assay (**Figure 5E**). Finally, as shown in **Figures 5F–J**, fibrosis markers and relative signaling pathways were examined at the protein and mRNA levels, all of which supported that miR-130a-3p could regulate cell differentiation by targeting TGF-βRII.

To further gain evidence regarding miR-130a-3p directly targeted TGF-βRII, we cotransfected NC and the miR-130a-3p mimic (Mimic) into H441 cells with a luciferase reporter system containing the wild-type (WT) or mutated (Mut) 3′-UTR of TGF-βRII (**Figures 6A,B**). The luciferase activity was decreased in H441 cells cotransfected with miR-130a-3p mimic and TGF-βRII-WT (Mimic + WT), compared with H441 cells cotransfected with NC and TGF-βRII-WT (NC + WT). However, the expression of TGF-βRII-Mut (Mimic + Mut) was not suppressed. These data suggest that TGF-βRII is a direct target gene of miR-130a-3p, which could regulate the differentiation of lung fibroblasts by directly interacting with the 3′-UTR of TGF-βRII.

MiR-130a-3p is Transferred to MLg When Co-Cultured With BMSCs

There is increasing evidence that miRNAs secreted by MSCs play their roles by entering into the receptor cells. We transfected miR-130a-3p mimic or NC into BMSCs, then collected BMSCs-CM after 24 h, and verified the expression of miR-130a-3p in BMSCs-CM by

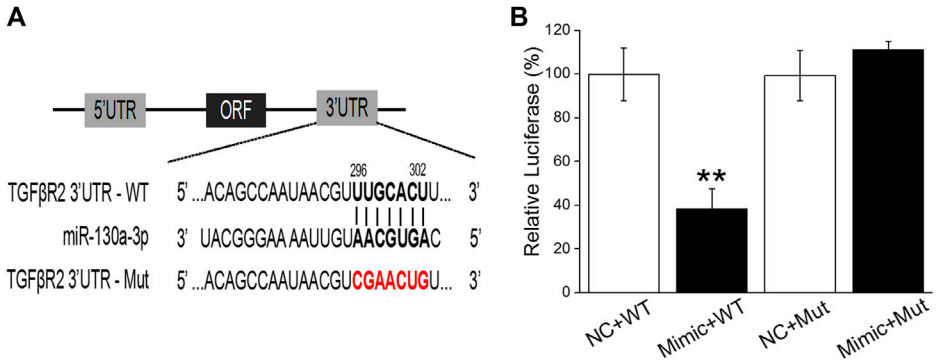

FIGURE 6 | TGF-βRII is a one of target genes of miR-130a-3p. **(A)** The possible binding sites of miR-130a-3p with TGF-βRII-3′UTR. **(B)** Dual-luciferase reporter assays of miR-130a-3p and TGF-βRII. Data were presented as mean ± SE, $^{**}p < 0.01$, compared with NC + WT group. $n = 3$.

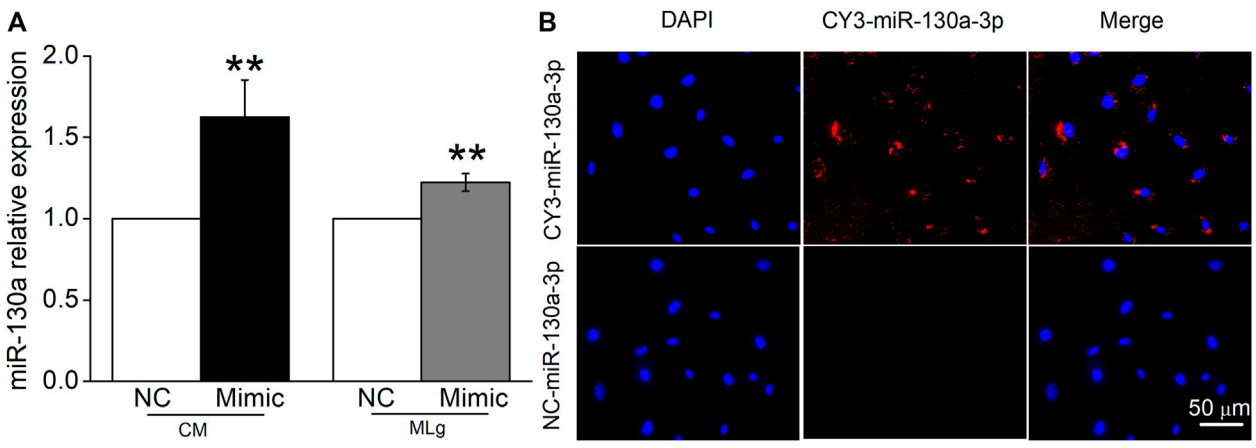

FIGURE 7 | MiR-130a-3p can be transferred to MLg co-cultured with BMSC. **(A)** MiR-130a-3p mimic (Mimic) or negative control (NC) was transfected in BMSCs, and the transfection efficiency was shown in BMSCs-CM (CM) and co-cultured MLg (MLg), respectively. **(B)** BMSCs were transfected with CY3-miR-130a-3p, and co-cultured with MLg for 24 h. The Nuclei were counterstained with DAPI (blue), and a representative CY3-miR-130a-3p stained image was shown in the MLg (red). Scale bar, 50 μm. Data were expressed as mean ± SE, $^{**}p < 0.01$, compared with NC group. $n = 3$–6.

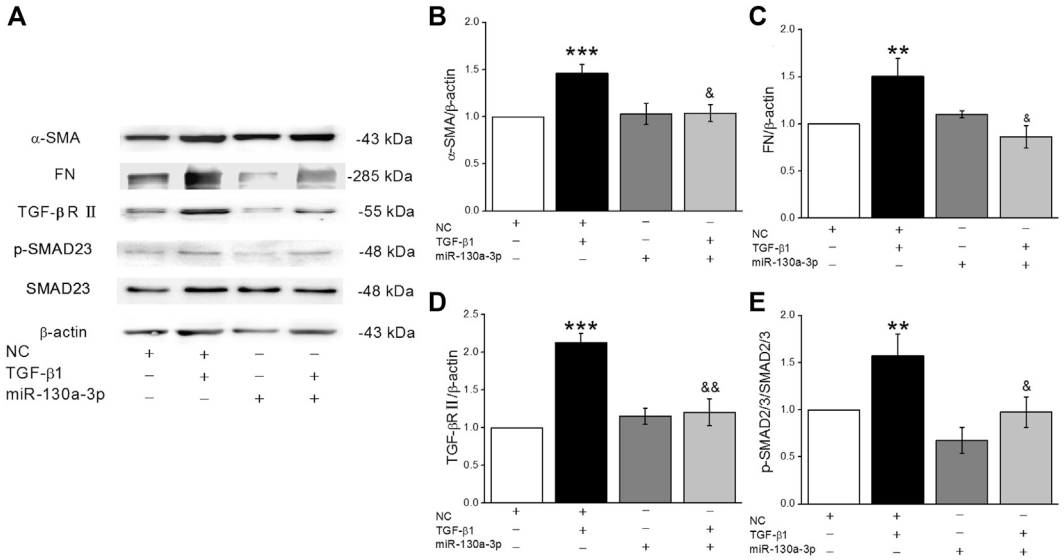

FIGURE 8 | MiR-130a-3p in BMSCs regulates fibrogenesis of MLg induced by TGF-β1 by inhibiting the function of TGF-βRII. **(A)** Representative Western blot bands of α-SMA, FN, TGF-βRII, Smad2/3 and p-Smad2/3 protein expression in BMSCs transfected with NC or miR-130a-3p mimic, followed by co-cultured with MLg. **(B–E)** The statistical analysis of the above-mentioned proteins was obtained from the relative gray values of the protein bands (α-SMA/β-actin, FN/β-actin, TGF-βRII/β-actin, p-Smad2/3/Smad2/3). Data were presented as mean ± SE, $^{**}p < 0.01$, $^{***}p < 0.001$, compared with NC group. $^{\&}p < 0.05$, $^{\&\&}p < 0.01$, compared with NC + TGF group. n = 3–4.

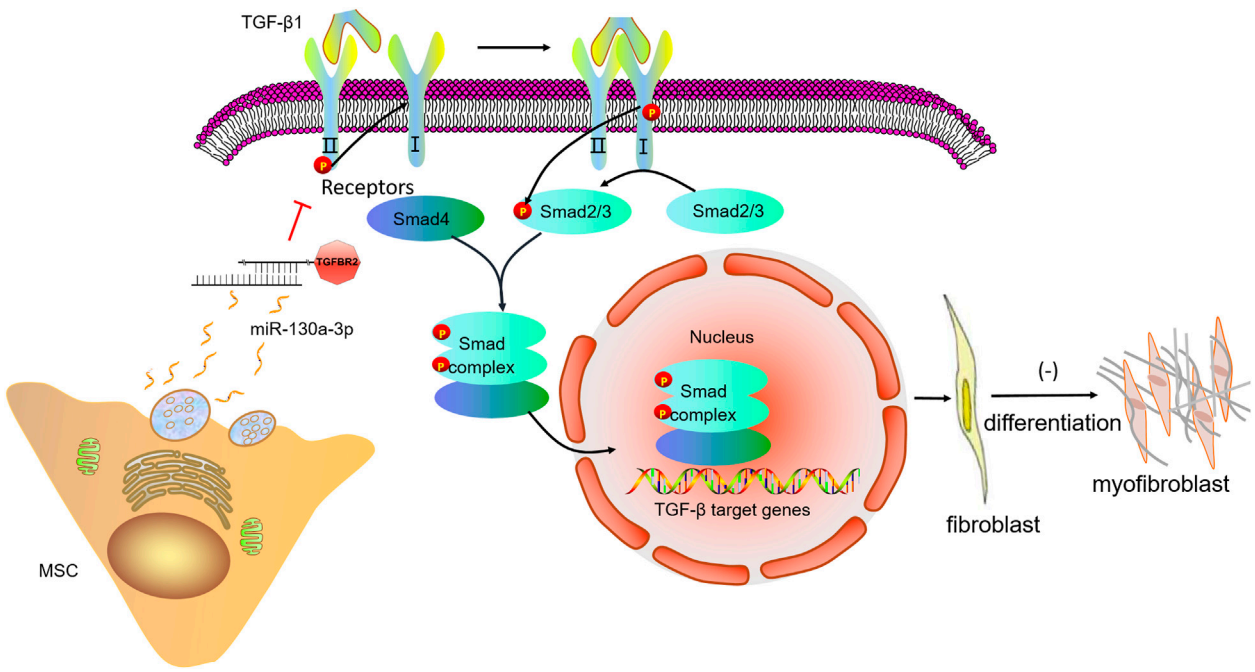

FIGURE 9 | A schematic diagram highlighting the regulation of the cell differentiation by miR-130a-3p in MSCs. The miR-130a-3p secreted by MSCs directly binds to the 3′UTR of TGF-βRII, thereby down-regulating TGF-βRII and inhibiting the recruitment and activation of TGF-βRI, subsequently, phosphorylation of Smad2/3 is inhibited, and unable to form a complex with Smad4, which translocates to the nucleus to regulate gene transcription. MSC, mesenchymal stem cells; TGF-β1, transforming growth factor-β1; TGFBR2, transforming growth factor-β receptor II.

qRT-PCR. Meanwhile, the transfected BMSCs were co-cultured with MLg, and the expression of miR-130a-3p was also detected in MLg (**Figure 7A**). In order to provide direct evidence that miR-130a-3p in BMSCs can be transferred to MLg, we transfected fluorescently labeled CY3-miR-130a-3p into BMSCs and observed its distribution in the co-cultured MLg under a fluorescence microscope. The evidence of CY3-miR-130a-3p appearance in MLg co-cultured with BMSCs, provided us a proof that at least miR-130a-3p from BMSCs could be transferred to the receptor cell MLg, and then exerted its effects on PF (**Figure 7B**).

MiR-130a-3p from BMSCs Participates in the Regulation of Fibrosis Through the TGF-β1/Smad Signaling Pathway

To investigate whether miR-130a-3p from BMSCs could ameliorate the expression of fibrosis markers, we transfected the miR-130a-3p mimic into BMSCs, which were then co-cultured with MLg. As shown in **Figure 8** A-E, MLg treated with TGF-β1 increased expression of α-SMA, FN, TGF-βRII, and p-SMAD2/3, all of which were reversed after administration of miR-130a-3p. The above data suggested that BMSCs may participate in the development of PF through miR-130a-3p, which could regulate the TGF-β1/Smad signaling pathway by targeting TGF-βRII.

DISCUSSION

PF is a progressive interstitial pneumonia characterized by excessive proliferation of fibroblasts and deposition of the extracellular matrix. Currently, the overall prognosis is poor, and effective therapeutic strategies are scarce (Noble et al., 2012; Wang et al., 2016; Chanda et al., 2019). Fibroblasts are regarded as the key effector cells of PF, involved in the key process of pathogenesis (Wuyts et al., 2013). Among them, TGF-β1/Smad signaling participates in the lung epithelium mesenchyme transition, and contributes to the process of PF (Saito et al., 2018b; Liu et al., 2018). In recent years, there has been much enthusiasm regarding MSC therapy for the treatment of lung diseases (Srour and Thébaud, 2015), and there are reports that the beneficial effects of MSCs may be mediated mainly through paracrine action (Willis et al., 2018). In this study, we first demonstrated the impact of BMSCs on MLg with Western Blot and qRT-PCR, and the results showed that compared with the control group, the expression of fibrosis marker and TGF-β1/Smad signaling pathway proteins and mRNAs increased in MLg after using TGF-β1 alone, whereas the effect was opposite after the coadministration of BMSCs. These results confirmed that BMSCs may contribute to alleviating fibrosis formation during PF, the mechanism of which is related to the regulation of the TGF-β1/Smad signaling pathway.

MiRNAs function by binding to the 3′-untranslated regions of mRNA to regulate posttranscriptional processes, thereby controlling various cellular processes (Su et al., 2015; Kang, 2017). We speculate that the above results may also work through miRNAs and evaluate the role of miR-130a-3p, which has been reported to reduce cell senescence and regulate the epithelial-mesenchymal transition (Jiang et al., 2020; Yin et al., 2020). However, it has been relatively seldom studied in TGF-β1-induced lung fibroblasts or PF. First, we confirmed the expression of miR-130a-3p in BMSC-CM and BMSCs by qRT-PCR. In addition, miR-130a-3p was downregulated by treatment with TGF-β1 in MLg, and when co-cultured with BMSCs, the expression level was significantly increased, suggesting that miR-130a-3p derived from BMSCs could influence TGF-β1-induced MLg. Next, overexpression of miR-130a-3p inhibited the cell differentiation phenotype. Future studies are warranted to explore the *in vivo* effects of miR-130a-3p in a bleomycin-induced PF animal model and its translational value as a diagnostic marker and therapeutic target for PF.

Of note, TGF-βRII has been predicted by relevant websites and verified as a potential target of miR-130a-3p using dual-luciferase reporter system in our study. Moreover, TGF-βRII was downregulated after miR-130a-3p overexpression, consistent with the direct targeting role of TGF-βRII for miR-130a-3p. Previous studies have shown that TGF-βRII-deficient mice could effectively resist PF caused by bleomycin (Li et al., 2011), supporting that as a receptor necessary for TGF-β1 signaling, TGF-βRII is essential for the development of PF (Li et al., 2011; Zhang et al., 2017). After the induction model was constructed by transfection of TGF-βRII siRNA, we found that cell differentiation were inhibited, and the expression of fibrosis marker proteins and mRNAs was reduced, indicating that silencing TGF-βRII had similar effects on the overexpression of miR-130a-3p in the process of affecting fibroblasts. We also verified that BMSCs transmit miR-130a-3p into TGF-β1-induced MLg to target the TGF-βRII axis, thereby inactivating the TGF-β1/Smad signaling pathway (**Figure 9**), which may provide a future direction for the treatment of PF.

CONCLUSION

MiR-130a-3p in BMSCs inhibits the lung fibroblast differentiation through blocking the activation of TGF-β1/Smad signaling pathway.

DATA AVAILABILITY STATEMENT

The raw data supporting the conclusion of this article will be made available by the authors, without undue reservation.

ETHICS STATEMENT

The animal study was reviewed and approved by the China Medical University.

AUTHOR CONTRIBUTIONS

Conceived and designed the study: YC and HN. Performed the study: YL and YD. Analyzed the data: YL, YH, and TY. Drafted the manuscript: YL and YC. Revised the draft of manuscript: HN. All authors corrected and approved the final version of the manuscript.

FUNDING

This work was supported by National Natural Science Foundation of China (NSFC 81670010).

REFERENCES

Aschner, Y., and Downey, G. P. (2016). Transforming Growth Factor-β: Master Regulator of the Respiratory System in Health and Disease. *Am. J. Respir. Cell Mol Biol* 54 (5), 647–655. doi:10.1165/rcmb.2015-0391tr

Asgarpour, K., Shojaei, Z., Amiri, F., Ai, J., Mahjoubin-Tehran, M., Ghasemi, F., et al. (2020). Exosomal microRNAs Derived from Mesenchymal Stem Cells: Cell-To-Cell Messages. *Cell Commun Signal* 18 (1), 149. doi:10.1186/s12964-020-00650-6

Barrett, C. S. X., Millena, A. C., and Khan, S. A. (2017). TGF-β Effects on Prostate Cancer Cell Migration and Invasion Require FosB. *Prostate* 77 (1), 72–81. doi:10.1002/pros.23250

Behnke, J., Kremer, S., Shahzad, T., Chao, C.-M., Böttcher-Friebertshäuser, E., Morty, R. E., et al. (2020). MSC Based Therapies-New Perspectives for the Injured Lung. *J. Clin. Med.* 9 (3), 682. doi:10.3390/jcm9030682

Boateng, E., and Krauss-Etschmann, S. (2020). miRNAs in Lung Development and Diseases. *Int. J. Mol. Sci.* 21 (8), 2765. doi:10.3390/ijms21082765

Chanda, D., Otoupalova, E., Smith, S. R., Volckaert, T., De Langhe, S. P., and Thannickal, V. J. (2019). Developmental Pathways in the Pathogenesis of Lung Fibrosis. *Mol. Aspects Med.* 65, 56–69. doi:10.1016/j.mam.2018.08.004

Chen, T. S., Lai, R. C., Lee, M. M., Choo, A. B. H., Lee, C. N., and Lim, S. K. (2010). Mesenchymal Stem Cell Secretes Microparticles Enriched in Pre-microRNAs. *Nucleic Acids Res.* 38 (1), 215–224. doi:10.1093/nar/gkp857

Cho, S. J., Lee, M., Stout-Delgado, H. W., and Moon, J.-S. (2020). DROSHA-Dependent miRNA and AIM2 Inflammasome Activation in Idiopathic Pulmonary Fibrosis. *Int. J. Mol. Sci.* 21 (5), 1668. doi:10.3390/ijms21051668

Dutta, R. K., Chinnapaiyan, S., and Unwalla, H. (2019). Aberrant microRNAomics in Pulmonary Complications: Implications in Lung Health and Diseases. *Mol. Ther. - Nucleic Acids* 18, 413–431. doi:10.1016/j.omtn.2019.09.007

Ferguson, S. W., Wang, J., Lee, C. J., Liu, M., Neelamegham, S., Canty, J. M., et al. (2018). The microRNA Regulatory Landscape of MSC-Derived Exosomes: a Systems View. *Sci. Rep.* 8 (1), 1419. doi:10.1038/s41598-018-19581-x

Froidure, A., Marchal-Duval, E., Homps-Legrand, M., Ghanem, M., Justet, A., Crestani, B., et al. (2020). Chaotic Activation of Developmental Signalling Pathways Drives Idiopathic Pulmonary Fibrosis. *Eur. Respir. Rev.* 29 (158), 190140. doi:10.1183/16000617.0140-2019

Glaesel, K., May, C., Marcus, K., Matschke, V., Theiss, C., and Theis, V. (2020). miR-129-5p and miR-130a-3p Regulate VEGFR-2 Expression in Sensory and Motor Neurons during Development. *Int. J. Mol. Sci.* 21 (11), 3839. doi:10.3390/ijms21113839

Hou, Y., Zhou, Z., Liu, H., Zhang, H., Ding, Y., Cui, Y., et al. (2020). Mesenchymal Stem Cell-Conditioned Medium Rescues LPS-Impaired ENaC Activity in Mouse Trachea via WNK4 Pathway. *Curr. Pharm. Des.* 26 (29), 3601–3607. doi:10.2174/1381612826666200131141732

Huang, C., Xiao, X., Yang, Y., Mishra, A., Liang, Y., Zeng, X., et al. (2017). MicroRNA-101 Attenuates Pulmonary Fibrosis by Inhibiting Fibroblast Proliferation and Activation. *J. Biol. Chem.* 292 (40), 16420–16439. doi:10.1074/jbc.m117.805747

Jiang, X., Ruan, X. L., Xue, Y. X., Yang, S., Shi, M., and Wang, L. N. (2020). Metformin Reduces the Senescence of Renal Tubular Epithelial Cells in Diabetic Nephropathy via the MBNL1/miR-130a-3p/STAT3 Pathway. *Oxid Med. Cell Longev* 2020, 8708236. doi:10.1155/2020/8708236

Jin, H., Yoo, Y., Kim, Y., Kim, Y., Cho, J., and Lee, Y.-S. (2020). Radiation-Induced Lung Fibrosis: Preclinical Animal Models and Therapeutic Strategies. *Cancers* 12 (6), 1561. doi:10.3390/cancers12061561

Kang, H. (2017). Role of MicroRNAs in TGF-β Signaling Pathway-Mediated Pulmonary Fibrosis. *Int. J. Mol. Sci.* 18 (12), 2527. doi:10.3390/ijms18122527

Kavianpour, M., and Saleh, M. (2020). The Role of Mesenchymal Stromal Cells in Immune Modulation of COVID-19: Focus on Cytokine Storm. *Stem Cell Res Ther* 11 (1), 404. doi:10.1186/s13287-020-01849-7

Kushibiki, T., Nagata-Nakajima, N., Sugai, M., Shimizu, A., and Tabata, Y. (2005). Delivery of Plasmid DNA Expressing Small Interference RNA for TGF-β Type II Receptor by Cationized Gelatin to Prevent Interstitial Renal Fibrosis. *J. Controlled Release* 105 (3), 318–331. doi:10.1016/j.jconrel.2005.02.030

Li, H., Zhao, X., Shan, H., and Liang, H. (2016). MicroRNAs in Idiopathic Pulmonary Fibrosis: Involvement in Pathogenesis and Potential Use in Diagnosis and Therapeutics. *Acta Pharmaceutica Sinica B* 6 (6), 531–539. doi:10.1016/j.apsb.2016.06.010

Li, M., Krishnaveni, M. S., Li, C., Zhou, B., Xing, Y., Banfalvi, A., et al. (2011). Epithelium-specific Deletion of TGF-β Receptor Type II Protects Mice from Bleomycin-Induced Pulmonary Fibrosis. *J. Clin. Invest.* 121 (1), 277–287. doi:10.1172/jci42090

Li, R.-F., Chen, X.-Y., Xu, Y., Feng, F.-C., He, H.-L., and Zhou, X.-M. (2021). Inhibitory Effects of Alkaline Extract from the Pericarp of Citrus Reticulata Blanco on Collagen Behavior in Bleomycin-Induced Pulmonary Fibrosis. *J. Ethnopharmacology* 269, 113761. doi:10.1016/j.jep.2020.113761

Li, S. N., and Wu, J. F. (2020). TGF-β/SMAD Signaling Regulation of Mesenchymal Stem Cells in Adipocyte Commitment. *Stem Cell Res Ther* 11 (1), 41. doi:10.1186/s13287-020-1552-y

Li, Z., Niu, S., Guo, B., Gao, T., Wang, L., Wang, Y., et al. (2020). Stem Cell Therapy for COVID-19, ARDS and Pulmonary Fibrosis. *Cell Prolif* 53 (12), e12939. doi:10.1111/cpr.12939

Liu, Y.-Y., Shi, Y., Liu, Y., Pan, X.-H., and Zhang, K.-X. (2018). Telomere Shortening Activates TGF-β/Smads Signaling in Lungs and Enhances Both Lipopolysaccharide and Bleomycin-Induced Pulmonary Fibrosis. *Acta Pharmacol. Sin* 39 (11), 1735–1745. doi:10.1038/s41401-018-0007-9

Liu, Y. L., Chen, B. Y., Nie, J., Zhao, G. H., Zhuo, J. Y., Yuan, J., et al. (2020). Polydatin Prevents Bleomycin-Induced Pulmonary Fibrosis by Inhibiting the TGF-β/Smad/ERK Signaling Pathway. *Exp. Ther. Med.* 20 (5), 62. doi:10.3892/etm.2020.9190

Marlina, M., Rahmadian, R., Armenia, A., Aviani, J. K., Sholihah, I. A., Kusuma, H. S. W., et al. (2021). Conditioned Medium of IGF1-Induced Synovial Membrane Mesenchymal Stem Cells Increases Chondrogenic and Chondroprotective Markers in Chondrocyte Inflammation. *Biosci. Rep.* 41 (7), BSR20202038. doi:10.1042/bsr20202038

Moghaddam, A. S., Afshari, J. T., Esmaeili, S.-A., Saburi, E., Joneidi, Z., and Momtazi-Borojeni, A. A. (2019). Cardioprotective microRNAs: Lessons from Stem Cell-Derived Exosomal microRNAs to Treat Cardiovascular Disease. *Atherosclerosis* 285, 1–9. doi:10.1016/j.atherosclerosis.2019.03.016

Noble, P. W., Barkauskas, C. E., and Jiang, D. (2012). Pulmonary Fibrosis: Patterns and Perpetrators. *J. Clin. Invest.* 122 (8), 2756–2762. doi:10.1172/jci60323

Saito, A., Horie, M., Micke, P., and Nagase, T. (2018a). The Role of TGF-β Signaling in Lung Cancer Associated with Idiopathic Pulmonary Fibrosis. *Int. J. Mol. Sci.* 19 (11), 3611. doi:10.3390/ijms19113611

Saito, A., Horie, M., and Nagase, T. (2018b). TGF-β Signaling in Lung Health and Disease. *Int. J. Mol. Sci.* 19 (8), 2460. doi:10.3390/ijms19082460

Sauler, M., Bazan, I. S., and Lee, P. J. (2019). Cell Death in the Lung: the Apoptosis-Necroptosis axis. *Annu. Rev. Physiol.* 81, 375–402. doi:10.1146/annurev-physiol-020518-114320

Shi, Q., Wu, H., Li, Y., Shen, L., Tian, X., and Lin, T. (2020). Inhibition of Wilms' Tumor Proliferation and Invasion by Blocking TGF-β Receptor I in the TGF-β/Smad Signaling Pathway. *Biomed. Res. Int.* 2020, 8039840. doi:10.1155/2020/8039840

Srour, N., and Thébaud, B. (2015). Mesenchymal Stromal Cells in Animal Bleomycin Pulmonary Fibrosis Models: a Systematic Review. *Stem Cell Transl Med* 4 (12), 1500–1510. doi:10.5966/sctm.2015-0121

Su, S., Zhao, Q., He, C., Huang, D., Liu, J., Chen, F., et al. (2015). miR-142-5p and miR-130a-3p Are Regulated by IL-4 and IL-13 and Control Profibrogenic Macrophage Program. *Nat. Commun.* 6, 8523. doi:10.1038/ncomms9523

Wang, C., Gu, S., Cao, H., Li, Z., Xiang, Z., Hu, K., et al. (2016). miR-877-3p Targets Smad7 and Is Associated with Myofibroblast Differentiation and Bleomycin-Induced Lung Fibrosis. *Sci. Rep.* 6, 30122. doi:10.1038/srep30122

Wang, X.-M., Liu, X.-M., Wang, Y., and Chen, Z.-Y. (2021). Activating Transcription Factor 3 (ATF3) Regulates Cell Growth, Apoptosis, Invasion and Collagen Synthesis in Keloid Fibroblast through Transforming Growth Factor Beta (TGF-Beta)/SMAD Signaling Pathway. *Bioengineered* 12 (1), 117–126. doi:10.1080/21655979.2020.1860491

Willis, G. R., Fernandez-Gonzalez, A., Anastas, J., Vitali, S. H., Liu, X., Ericsson, M., et al. (2018). Mesenchymal Stromal Cell Exosomes Ameliorate Experimental Bronchopulmonary Dysplasia and Restore Lung Function through Macrophage Immunomodulation. *Am. J. Respir. Crit. Care Med.* 197 (1), 104–116. doi:10.1164/rccm.201705-0925oc

Wnuk, D., and Paw, M. (2020). Enhanced Asthma-Related Fibroblast to Myofibroblast Transition Is the Result of Profibrotic TGF-β/Smad2/3

Pathway Intensification and Antifibrotic TGF-β/Smad1/5/(8)9 Pathway Impairment. *Sci. Rep.* 10 (1), 16492. doi:10.1038/s41598-020-73473-7

Wolters, P. J., Collard, H. R., and Jones, K. D. (2014). Pathogenesis of Idiopathic Pulmonary Fibrosis. *Annu. Rev. Pathol. Mech. Dis.* 9, 157–179. doi:10.1146/annurev-pathol-012513-104706

Wu, Q., and Xu, Y. (2020). A Clinical Model for the Prediction of Acute Exacerbation Risk in Patients with Idiopathic Pulmonary Fibrosis. *Biomed. Res. Int.* 2020, 8848919. doi:10.1155/2020/8848919

Wuyts, W. A., Agostini, C., Antoniou, K. M., Bouros, D., Chambers, R. C., Cottin, V., et al. (2013). The Pathogenesis of Pulmonary Fibrosis: a Moving Target. *Eur. Respir. J.* 41 (5), 1207–1218. doi:10.1183/09031936.00073012

Yang, J., Pan, X., Wang, L., and Yu, G. (2020). Alveolar Cells under Mechanical Stressed Niche: Critical Contributors to Pulmonary Fibrosis. *Mol. Med.* 26 (1), 95. doi:10.1186/s10020-020-00223-w

Yin, J., Ye, Y.-L., Hu, T., Xu, L.-J., Zhang, L.-P., Ji, R.-N., et al. (2020). Hsa_circRNA_102610 Upregulation in Crohn's Disease Promotes Transforming Growth Factor-β1-Induced Epithelial-Mesenchymal Transition via Sponging of Hsa-miR-130a-3p. *World J. Gastroenterol.* 26 (22), 3034–3055. doi:10.3748/wjg.v26.i22.3034

Yoshida, K., Matsuzaki, K., Murata, M., Yamaguchi, T., Suwa, K., and Okazaki, K. (2018). Clinico-Pathological Importance of TGF-β/Phospho-Smad Signaling During Human Hepatic Fibrocarcinogenesis. *Cancers* 10 (6), 183. doi:10.3390/cancers10060183

Zhang, Q., Ye, H., Xiang, F., Song, L.-J., Zhou, L.-L., Cai, P.-C., et al. (2017). miR-18a-5p Inhibits Sub-pleural Pulmonary Fibrosis by Targeting TGF-β Receptor II. *Mol. Ther.* 25 (3), 728–738. doi:10.1016/j.ymthe.2016.12.017

Zhi, N., Mo, Q., Yang, S., Qin, Y. X., Chen, H., Wu, Z. G., et al. (2020). Treatment of Pulmonary Fibrosis in One Convalescent Patient with corona Virus Disease 2019 by Oral Traditional Chinese Medicine Decoction: A Case Report. *J. Integr. Med.* 5, S2095–S4964. doi:10.1016/j.joim.2020.11.005

Zhong, G., Lin, Y., Wang, X., Wang, K., Liu, J., and Wei, W. (2020). H19 Knockdown Suppresses Proliferation and Induces Apoptosis by Regulating miR-130a-3p/SATB1 in Breast Cancer Cells. *Onco Targets Ther.* 13, 12501–12513. doi:10.2147/ott.s280142

Zhou, Z., Hua, Y., Ding, Y., Hou, Y., Yu, T., Cui, Y., et al. (2021). Conditioned Medium of Bone Marrow Mesenchymal Stem Cells Involved in Acute Lung Injury by Regulating Epithelial Sodium Channels via miR-34c. *Front. Bioeng. Biotechnol.* 9, 640116. doi:10.3389/fbioe.2021.640116

Conflict of Interest: The authors declare that the research was conducted in the absence of any commercial or financial relationships that could be construed as a potential conflict of interest.

Publisher's Note: All claims expressed in this article are solely those of the authors and do not necessarily represent those of their affiliated organizations, or those of the publisher, the editors and the reviewers. Any product that may be evaluated in this article, or claim that may be made by its manufacturer, is not guaranteed or endorsed by the publisher.

Copyright © 2021 Liu, Ding, Hou, Yu, Nie and Cui. This is an open-access article distributed under the terms of the Creative Commons Attribution License (CC BY). The use, distribution or reproduction in other forums is permitted, provided the original author(s) and the copyright owner(s) are credited and that the original publication in this journal is cited, in accordance with accepted academic practice. No use, distribution or reproduction is permitted which does not comply with these terms.